Audio Engineering Society

Conference Paper 11

Presented at the International Conference on Acoustics & Sound Reinforcement
2024 January 22–26, Le Mans, France

The loudspeaker as a sustainable and aesthetic product using additive manufacturing

Manuel Isenegger[1], Elias Schedler[1], Verena Hutter[2], Christoph Zumbühl[1], Othmar Schälli[3], and Armin Taghipour[1]

[1]*Lucerne School of Engineering and Architecture, Lucerne University of Applied Sciences and Arts, Horw, Switzerland*
[2]*Verena Hutter, Zurich, Switzerland*
[3]*Pure Sonic GmbH, Walchwil, Switzerland*

Correspondence should be addressed to Manuel Isenegger (manuel.isenegger@hslu.ch)

ABSTRACT

State-of-the-art loudspeaker development is mainly motivated by added functionality and improved audio quality. Consequently, innovations are typically located in the field of signal processing and electronics. In contrast, the loudspeaker design presented here is inspired by three main concepts: additive manufacturing, aesthetic design and sustainability. Initially, a prototype developed by Verena Hutter established a benchmark. This project focused on the possibilities of broadband sound radiation in an aesthetic cabinet with a secluded driver. To achieve an even spatial sound distribution, different reflective elements were produced and their respective frequency response at different listening positions was measured. Considering the limitations given by the additive manufacturing process and material, as well as the aesthetic vision of a Möbius ring, a cabinet was designed and electroacoustically optimized with a commercially available driver. To improve sustainability, the electronics were optimized for energy efficiency. Moreover, the possibility to easily disassemble and thus repair or replace different parts of the loudspeaker was included into the design. The project resulted in an aesthetically pleasing, 3D-printed loudspeaker out of sustainable material with a secluded driver, a wide frequency range, improved energy efficiency, and simple disassembly.

1 Introduction

Loudspeaker cabinets are traditionally assembled from various parts and materials, and, subsequently, joined using different techniques, usually bolted or glued connections. This production process has its inherent limitations in terms of possible geometries. More complex cabinet geometries can be achieved using mold casting, which in turn has different limitations, as well as higher cost per unit, especially for low production volumes.
Additive manufacturing (also known as “3D-printing”) is increasing in popularity, especially since new and/or complex geometries can easily be designed and produced with this method. The additive manufacturing process is used in different technical [1] as well as artistic applications [2]. Recently, also in loudspeaker production [3, 4].
Current loudspeaker cabinet production often uses materials, which contain harmful chemicals or can only be reused or recycled under considerable material separation and energy efforts [5]-[10]. Furthermore, modern loudspeaker assembly often does not allow repair or

Fig. 1: Initial silicon carbide prototype with driver at bottom position and no reflective element.

replacement of parts. Due to climate change and waste disposal challenges, sustainability is a key factor in production processes today, to which the loudspeaker industry can contribute by including sustainable, recyclable choices of materials and the possibility to repair or replace different parts of a loudspeaker.
The loudspeaker presented here was created using additive manufacturing with the aim of pleasing aesthetics, sustainability and competitive audio specifications.

2 Prior to the project

The initial prototype featured a midrange woofer with a transmission line-type cabinet, developed by Verena Hutter in her Masters Thesis at Bang & Olufsen. The frequency range of this loudspeaker extends from 100 to 3'000 Hz and established a benchmark. The narrow frequency range and low maximum sound pressure level (SPL) were the main drawbacks of this prototype. Additional targets for optimization were the distortions caused by loose joints as well as the radiation inefficiency due to the driver's placement close to the surface below.

3 Additive manufacturing

3.1 Materials

The material choice for the initial prototype was silicon carbide (SiSiC) in accordance with Bang & Olufsen's design directive for ceramic materials. The acoustic characteristics of this cabinet material were expected to compare well with traditional materials, especially due to the material's high stiffness. However, a significant drawback associated with silicon carbide is its limited availability in additive manufacturing, with only two suppliers operating within Europe. Furthermore, the material's production necessitates substantial amounts of energy [11]. In contrast, 3D-printed quartz sand as the primary source material offers ease of procurement and sustainability in its production. Quartz sand resources are large [12] and 3D-printing using this material requires little energy as no additional heating is involved in the process [13]. The transition from silicon carbide to sand within this project led to an overall reduction in production energy requirements. Notably, the source material's recyclability is improved, given its reuse in subsequent printing processes. The stiffness of the sand-based material is expected to be comparable to that of silicon carbide, hence, also its expected acoustic performance. Both printing materials show robustness against temperature changes (deformation, combustion, etc.). However, both materials exhibit a high acoustic reflection coefficient. Therefore, internal damping of the cabinet is necessary to mitigate reflections and standing waves.

3.2 Geometry

Besides energy efficiency and recyclability, the aesthetic design was a core target of this project. The Möbius shape was selected as a visual representation of the wave propagation. It serves to metaphorically convey a sense of limitless continuity, parallel to the immersive nature of sound. From a construction perspective, this geometry exhibits inherent self-supporting attributes, rendering the inclusion of supplementary pillars or internal reinforcements unnecessary. This design characteristic gains particular significance when adjusting the size of the unit. Consequently, the geometry contributes to a judicious employment of production materials.
Furthermore, utilization of computer aided design (CAD) allows for a fast and relatively simple conception of new geometries. Typical problems with classical production processes (e.g. internal sharp edges, which can induce audible turbulence) can be mitigated with a few clicks in the CAD software and do not unnecessarily prolong the production process. The same is valid for other complex internal structures.

4 Electroacoustical optimization

4.1 Technical requirements

The loudspeaker optimization was given the following technical design goals:

- Frequency Response (-3 dB): 50 – 20'000 Hz
- Max. broadband SPL at 1 m distance (Total Harmonic Distortion + Noise < 5%): 85 dB
- Active amplification (amplification module inside cabinet)

4.2 Driver

A single driver was chosen to emit the whole of the desired frequency range for three reasons. Firstly, the non-visibility requirement with regard to the driver only leaves the bottom of the structure for placement. Secondly, the available surface at the bottom of the desired geometry is sufficient for only one driver. A third reason is linked to the reflective elements and described in section 4.4.
In order to attain the given technical requirements, a commercially available driver, capable of reproducing the required frequency response was selected according to availability and indications in the respective data sheets. The selected driver is a coaxial type and has the following technical specifications:

- Woofer:
  - Nominal Impedance: 4 Ω
  - DC resistance, Re 3.1 Ω
  - Voice coil diameter 25.4 mm
  - Voice coil height 15 mm
  - Air gap height 5 mm
  - Free air resonance, Fs 55 Hz
  - Sensitivity (2.83V/1m) 87.5 dB
  - Rated power handling 30 W
  - Magnetic flux density 1.03 T
- Tweeter:
  - Nominal Impedance 4 Ω
  - DC resistance, Re 3.0 Ω
  - Voice coil diameter 12.4 mm
  - Voice coil height 1.2 mm
  - Air gap height 1.5 mm
  - Free air resonance, Fs 1300 Hz
  - Sensitivity (2.83V/1m) 87.5 dB
  - Rated power handling 10 W
  - Magnetic flux density 0.97 T

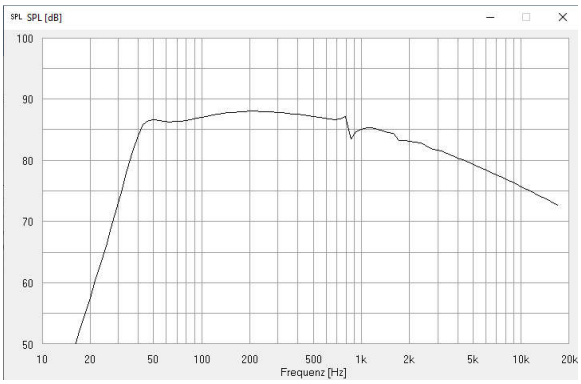

Fig. 2: Simulated magnitude frequency response of the woofer with optimized cabinet parameters.

4.3 Cabinet

As mentioned, the aesthetically desired geometry was determined to be a Möbius ring. Different cabinet types (closed, bass reflex, transmission line, horn) were considered, of which the bass reflex design was selected, because of its combination of simplicity in design and tuning, small volume requirements and its low frequency radiation efficiency [14]. The software programs WinISD (Version 0.7.0.950) and AJHorn (Version 7.0.2971), were used to simulate and optimize the cabinet parameters (rear volume in liters, bass reflex channel cross-sectional area, bass reflex channel length). The Thiele Small parameters of the selected driver were entered in the software, and the cabinet parameters were optimized for an even frequency response. The software predicted a lower limit of the frequency range of around 40 Hz. See Fig. 2 for the simulated magnitude frequency response of the woofer-part of the coaxial driver.

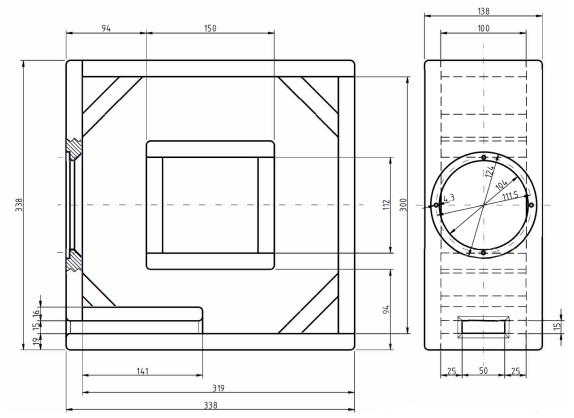

Fig. 3: Plans of intermediate prototype with driver at bottom position.

The optimized cabinet parameters were calculated to be as follows:

- Rear volume 5.3 l
- Bass reflex channel cross-sectional area 7.5 cm^2
- Bass reflex channel length 16 cm

These parameters together with the dimensions of the driver defined the geometry of the Möbius ring.

To validate the simulations of the cabinet optimization, the selected driver was acquired and a simple, intermediate prototype with the optimized cabinet parameters built out of MDF-wood, resembling the intended design (square ring volume instead of Möbius ring volume). This prototype's geometry can be seen in Fig. 3.

Intermediate measurements with the prototype proved the accuracy of the simulations, as can be seen in Fig. 4. The SPL reduction above 3 kHz is due to measurement microphone's positioning in between driver axis and bass reflex axis. Acoustic measurements have been taken in the anechoic chamber of the Lucerne School of Engineering and Architecture (HSLU T&A), using the software "Room Equalization Wizard" (REW, Version 5.20.13).

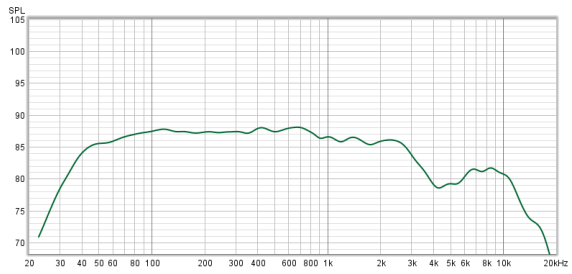

Fig. 4: Near-field magnitude frequency response (measurement position in between driver axis and bass reflex axis) of wooden intermediate prototype.

4.4 Reflective element

As mentioned, in order to seclude the driver from view, it was placed at the bottom of the Möbius ring volume with the driver axis oriented downwards. Due to the inherent loudspeaker directivity [15], this downward orientation reduces high frequency emission towards the listening positions around the loudspeaker, if there is no reflective surface beneath. To overcome this issue, a reflective element was included in the design. This decision represents the third reason for using a single driver, instead of a multi-way system (see Subsection 4.2). Using several drivers would require several reflective elements. The reflective element of the first driver would deflect the wanted reflections of the second driver for certain directions and vice versa.

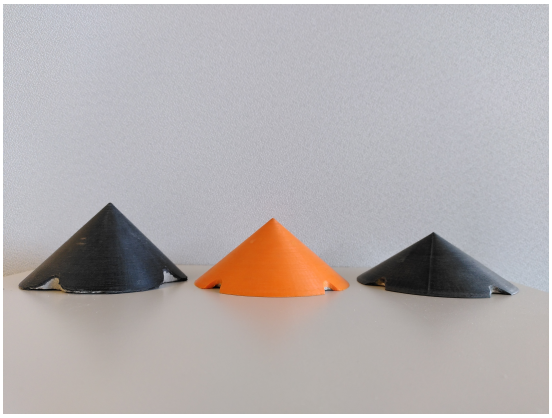

Fig. 5: Reflective elements in cone shape with different apertures (left: 90°, middle: 105°, right: 120°).

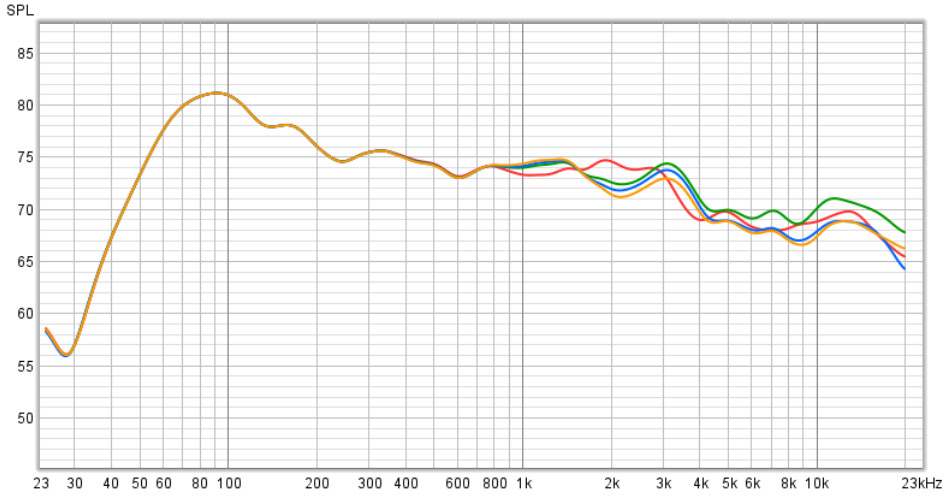

Fig. 6: Frequency responses of loudspeaker with different reflective elements underneath (red: no reflector, green: aperture = 120°, blue: aperture = 105°, orange: aperture = 90°) measured at typical listening position (2 m distance, 0° Azimuth, 40° Elevation).

As a simplification, the loudspeaker was assumed to be a point source, emitting spherical waves. A set of cone-shaped reflective elements exhibiting different apertures (90°, 105° and 120°, all with 6 cm base radius) was 3D-printed for testing; see Fig. 5. The conical shape was chosen, since it geometrically deflects and disperses the spherical waves emitted by the loudspeaker toward the listening positions [16]. The size of the base was chosen to allow for a specular reflection of (high) frequencies with wavelengths shorter than the diameter of the base. For (low) frequencies with wavelengths larger than the diameter of the base, a scattering effect occurs, reflecting less sound energy [16]. For even lower frequencies and larger wavelengths, the effect of the reflective element is expected to be completely negligible. The corresponding frequency, above which specular reflection occurs, is at around 3 kHz. This frequency, with the resulting base diameter, was chosen according to the magnitude frequency response data at different angles in the driver data sheet [17].

Intermediate measurements of the reflectors made with the wooden prototype showed variations in the magnitude frequency response between different reflective elements for a number of elevation angles. The magnitude frequency responses for the typical listening position at 40° elevation are depicted in Fig. 6. Only small differences occur due to the reflective elements. In addition, no clear trend toward a better high frequency coverage is visible with the reflective elements compared to the case with no reflective element. Rather constructive and destructive interference create a comb-filter effect. This, it was estimated, was due to the small surface of the reflective elements, which was insufficient to effectively divert high frequency energy toward the listener. This motivated the decision for a larger reflective surface in the final prototype, which was expected to divert more high frequency sound toward the listener.

5 Development of electronics

5.1 State-of-the-art commercial solution

Commercial speaker electronics of compact speakers usually include a data exchange interface for transferring wireless data from external audio sources. The Bluetooth standard or WLAN are often used for this purpose. The received audio signal is then transmitted to the amplifier in digital or analog form, where it is amplified for the speaker's driver. Commercial solutions often include additional signal processing functionalities and algorithms. As a reference for this project, a Dayton KABD-250 2x50 W Amplifier Board with DSP and Bluetooth was used.

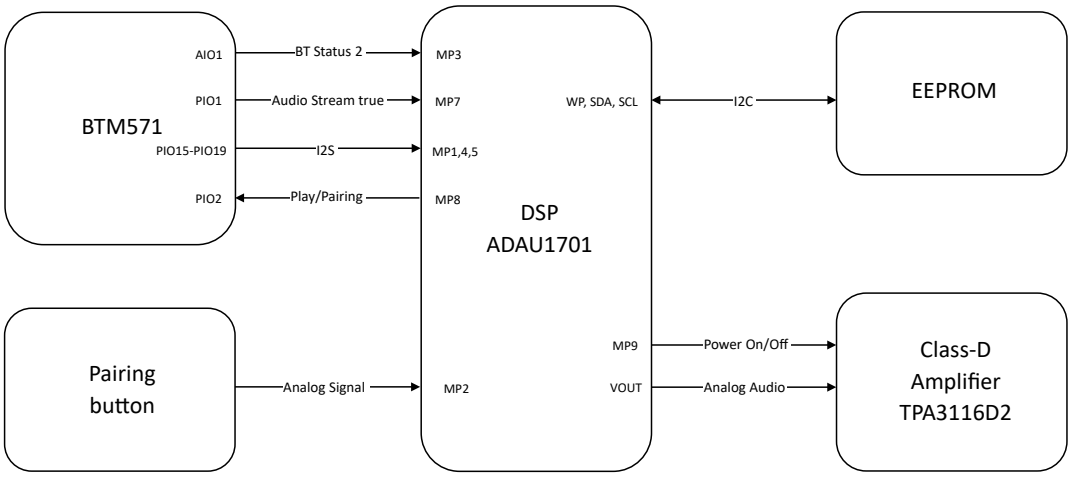

Fig. 7: Schematic of the electronic components

Fig. 8: PCB mounted on the back of the driver

5.2 Electronic development

During the development of the loudspeaker electronics, the aspects of clean audio data transmission via Bluetooth, digital signal processing (DSP) and amplification were considered. A different aspect to be taken into account was the energy consumption, especially in standby-mode, compared to commercially available products. A Dayton audio amplifier board was used as a reference for this project.

5.2.1 Electronic circuit

A schematic of the electronic layout can be seen in Fig. 7. A Bluetooth module with Bluetooth standard 5.3 was chosen as a receiving device. This was connected to the DSP via I^2S protocol. The stereo audio signal is transmitted with a sampling rate of 44.1 kHz, then mixed to mono and fed into a crossover network (with a woofer-tweeter crossover frequency at 2 kHz) in the DSP. For amplification, a Class-D amplifier (TPA3118D2) with a power of 2x30 W RMS was used. The data exchange between digital signal processor (DSP) and the amplifier is analog. To avoid electromagnetic interference, an additional filter was implemented at the output stage.

5.2.2 Printed circuit board design

The printed circuit board (PCB) design was chosen to be round in order to easily fit on the back of the loudspeaker driver (see Fig. 8). Doing so, no additional material is necessary for mounting and disassembling the PCB. This arrangement also allows the electronics hardware to be used in any number of different loudspeaker cabinets.

5.2.3 Bluetooth module

The Bluetooth module (BTM571) is made by Qualcomm (Chip: QCC30XX v5.0), which comes with features such as True Wireless Mirroring and Low Latency. With the Bluetooth 5.3 standard, the speaker is thus on the cutting edge of Bluetooth technology and offers many functional possibilities.

Fig. 9: Final prototype 3D-printed from sand as a source material with driver at bottom position and larger reflective element on pedestal.

5.2.4 Energy efficiency

To maximize energy efficiency in standby-mode, care has been taken to ensure that all other electrical systems switch off, when no user is connected to the speaker's Bluetooth module. A threshold detection of the Bluetooth audio input signal sends a power-down signal to the amplifier, when there is no incoming audio signal (see Fig. 7). When a Bluetooth audio signal is present, a power-up signal is sent to the loudspeaker. Standby power consumption was thus reduced by 80% from 1.6 W to 0.34 W.

6 Results

6.1 Final prototype

The design of the final prototype (Fig. 9) was informed by the knowledge gained in the preceding optimization process. A larger reflector area was chosen to increase the amount of reflected high frequency sound energy.

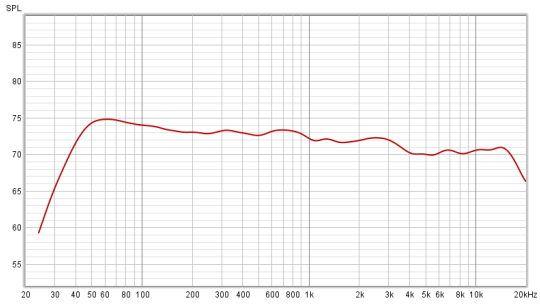

Fig. 10: Near field frequency response (on axis with reference to the driver) of final prototype without reflective element.

Rounded edges inside the internal volume as well as for the bass-reflex port were included to prevent turbulence noise. The bass-reflex port is from the same material as the rest of the cabinet and its curved form is directly included in the 3D-printing process. The curved form allows for the whole length to be included inside the loudspeaker volume. Other production processes would not have allowed this, unless additional assembly steps were included. Additional internal structures for the reduction of standing waves were beyond the scope of this project. Furthermore, a pedestal was built, containing a USB-C power supply socket in the metal base, four thin metal rods holding the loudspeaker, two of which are conducting the current from the power supply to the electronics inside the speaker.

The loudspeaker was designed, such that every component can be removed with common tools found in standard toolboxes. As no parts are glued to each other, broken parts can be easily repaired or replaced, without having to replace the whole product. Thus, unnecessary disposal of functional parts is prevented.

6.2 Electrical measurements

The electrical measurements included distortion measurements, power measurements, latency measurements and a temperature measurement. In the distortion measurement of the system "Bluetooth-Module, DSP, and Amplifier", a Total Harmonic Distortion and Noise (THD+N) of 0.07% was measured at a power of 1 Watt and a frequency of 1 kHz. Furthermore, a maximum power of 3.22 W was observed during the power measurement. The standby consumption was 340 mW. The latency measurement showed a latency between the

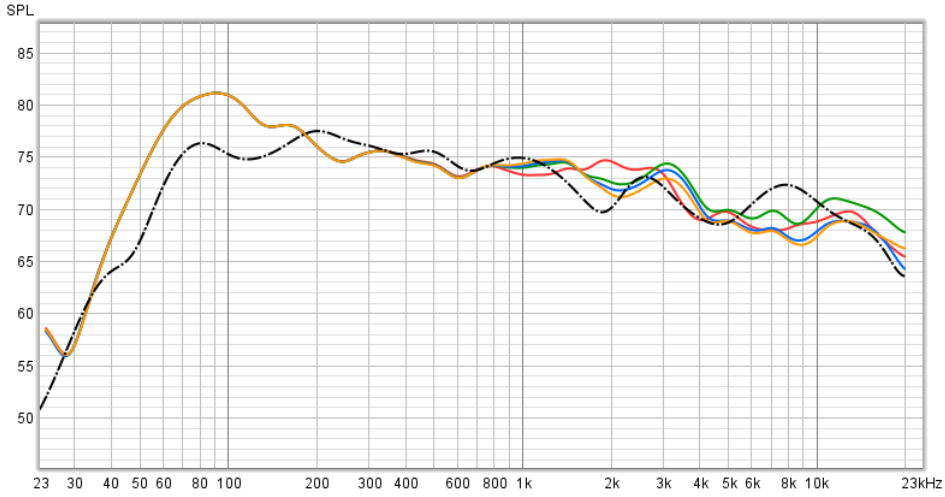

Fig. 11: Frequency responses of Fig. 6 with additional dash-dotted black curve representing final loudspeaker with larger reflective element underneath.

playing device and the loudspeaker of 148 ms. The temperature measurement, carried out at the maximum power of 3.22 W, resulted in a hotspot temperature of 51.8° C at the DSP.

6.3 Acoustic measurements

The final prototype was measured in the anechoic chamber of the Lucerne School of Engineering and Architecture (HSLU T&A). Its near field magnitude frequency response can be seen in Fig. 10. No drop-off at higher frequencies is seen, because the measurement position is on axis with reference to the driver, whereas in the case of the intermediate prototype, the measurement position in Fig. 4 was off axis with reference to the driver.

The lower cut-off frequency lies below 40 Hz and an even frequency distribution is achieved in the near field of the loudspeaker.
Fig. 11 shows the same magnitude frequency responses as in Fig. 6 with the addition of the final prototype featuring a larger reflective element (8 cm base radius). It should be noted that no additional digital audio equalization was used in this measurement. The observed differences in the lower frequency distribution are assumed to arise from differences in cabinet geometry and material properties (square ring versus Möbius ring volume, MDF versus sand). The small increase in reflection area is assumed to cause the slight SPL increase around 7 kHz. However, due to interference between reflected and diffracted sound, SPL at other frequencies decreases compared to the case with smaller reflective elements.

The technical requirements regarding frequency response were met for the case of the on-axis measurement, but not for the measurement at the listening position. The requirement for maximum SPL at 1m distance was not fulfilled. For a sound pressure level of 80 dB at the listening position, using a broadband excitation signal, the driver arrives at its maximum linear coil travel distance. For this reason, a limiter was included in the algorithm, which did not allow the sound pressure level to go beyond this level. The active amplification requirement was satisfied.

7 Conclusions and outlook

7.1 Conclusions

Additive manufacturing was used as a basis for the creation of a loudspeaker, combining aesthetics, sustainability, and audiophile sound quality. The use of a reflective element allowed for the driver to be secluded from view, thus presenting the cabinet in the form of a Möbius ring as the central aesthetic element. The cabinet material was chosen so as to reduce the energy required for production, the use of scarce and harmful materials and to allow for recycling of the source

material. The geometry as well as the design of the PCB were optimized for simple disassembly, and thus repair. In addition, parts were designed such that no additional structures (and thus additional material) are necessary for mounting. The electronics were optimized for energy efficiency and a reduction of 80% in standby power consumption was achieved. The on-axis frequency response extends to below 40 Hz, the maximum SPL is limited to 80 dB and an active amplification topology was implemented.

7.2 Outlook

The additive manufacturing process allows for complex internal geometries. This possibility could be exploited further in order to create internal geometries and surfaces, which have a diffusive reflective behaviour, or reduce standing waves inside the cabinet.
The combination of the simple geometric cabinet requirements (volume, bass reflex channel cross-sectional area and bass reflex channel length) with additive manufacturing could be used to create manifold cabinet geometries and thus aesthetic visions.
A numerical simulation (e.g. with the Boundary Element Method, BEM) of the radiation behavior of the driver in combination with the reflective element would allow for optimization of the geometry of the reflective element [18, 19]. An optimal solution regarding frequency response at different listening positions should be investigated in future works.

Acknowledgments

This project was partially funded by Innosuisse (the Swiss Innovation Agency) via an innovation cheque (65154.1 INNO-ENG).
The authors would like to thank Frederik Imhof and Beat Bürgler for their valuable contributions regarding Bluetooth technology and the building of prototypes to this project.

References

[1] Haleem, A. and Javaid, M., "Additive manufacturing applications in industry 4.0: a review," *Journal of Industrial Integration and Management*, 4, p. 1930001, 2019.

[2] Zhu, J. and Liu, W., "Art Design of Ceramic Sculpture Based on 3D Printing Technology and Electrochemistry," *Journal of Chemistry*, 2022, 2022.

[3] Chojnacki, B., Pawlik, J., and Kamisinski, T., "Influence of different materials used for 3D printing in miniature speaker enclosure development," in *INTER-NOISE and NOISE-CON Congress and Conference Proceedings*, volume 263, pp. 5631–5636, Institute of Noise Control Engineering, 2021.

[4] Saari, M., Cox, B., Richer, E., Krueger, P. S., and Cohen, A. L., "Fiber encapsulation additive manufacturing: An enabling technology for 3D printing of electromechanical devices and robotic components," *3D Printing and Additive Manufacturing*, 2(1), pp. 32–39, 2015.

[5] Wilson, J. B., "Medium Density Fiberboard (MDF): A Life-cycle inventory of manufacturing panels from resource through product," *Final Report to the Consortium for Research on Renewable Industrial Materials*, 2008.

[6] Adeeb, E., Kim, T. W., and Sohn, C. H., "Cost-benefit analysis of medium-density fiberboard production by adding fiber from recycled medium-density fiberboard," *Forest Products Journal*, 68(4), pp. 414–418, 2018.

[7] Zimmer, A. and Bachmann, S. A. L., "Challenges for recycling medium-density fiberboard (MDF)," *Results in Engineering*, 19, p. 101277, 2023.

[8] Meekers, I., Refalo, P., and Rochman, A., "Analysis of process parameters affecting energy consumption in plastic injection moulding," *Procedia CIRP*, 69, pp. 342–347, 2018.

[9] Haraldsson, J. and Johansson, M. T., "Review of measures for improved energy efficiency in production-related processes in the aluminium industry–From electrolysis to recycling," *Renewable and Sustainable Energy Reviews*, 93, pp. 525–548, 2018.

[10] von Gries, N. and Bringezu, S., "Using New Spare Parts for Repair of Waste Electrical and Electronic Equipment? The Material Footprint of Individual Components," *Resources*, 11(2), p. 24, 2022.

[11] Wahl, L., Lorenz, M., Biggemann, J., and Travitzky, N., "Robocasting of reaction bonded silicon carbide structures," *Journal of the European Ceramic Society*, 39(15), pp. 4520–4526, 2019.

[12] U.S. Geological Survey, "Sand and Gravel (Industrial), Mineral Commodity Summaries, January 2023," https://pubs.usgs.gov/periodicals/mcs2023/mcs2023-sand-industrial.pdf, 2023, accessed: 11-29-2023.

[13] Sandhelden GmbH & Co. KG, "Frequently asked questions about the Manufacturing Process," https://www.sandhelden.de/about-us, 2023, accessed: 11-29-2023.

[14] Newell, P. and Holland, K., *Loudspeakers: for music recording and reproduction*, Routledge, 2018.

[15] Ballou, G., *Electroacoustic Devices: Microphones and Loudspeakers*, Routledge, Oxford, 2009, ISBN 0240812670.

[16] Kuttruff, H., *Room acoustics*, Taylor & Francis, London, 5th ed. edition, 2009, ISBN 9780415480215.

[17] SB Acoustics, "Data Sheet SB Acoustics 4" SB12PACR-4-COAX," https://sbacoustics.com/wp-content/uploads/2023/06/4in-SB12PACR25-4-COAX.pdf, 2023, accessed: 11-29-2023.

[18] Comsol Multiphysics GmbH, "Loudspeaker Radiation: BEM Acoustics Tutorial," https://www.comsol.de/model/loudspeaker-radiation-bem-acoustics-tutorial-59271, 2023, accessed: 09-21-2023.

[19] Esfahlani, H., Karkar, S., Lissek, H., and Mosig, J. R., "Acoustic dispersive prism," *Scientific reports*, 6(1), p. 18911, 2016.